

Supporting Information

Magnetron sputtering tuned “ π back-donation” sites over metal oxides for enhanced electrocatalytic nitrogen reduction

*Yuan Tian[#], Bin Chang^{#, *}, Guihua Wang, Lili Li, Lianguo Gong, Bo Wang, Rusheng Yuan and Weijia Zhou*

Email: chm_changb@ujn.edu.cn

This file includes:

S1. Materials

S2. Synthesis of NiO@TiO₂

S3. Physicochemical characterization

S4. Computational Details

S5. Electrochemical testing

S6. Determination of NH₃

S7. Calculations of NH₃ yield and Faradaic efficiency

S8. ¹⁵N isotope labeling experiments

S9. Supplementary figures and tables

S1. Materials

Tetrabutyl titanate, acetone and hydrochloric acid were purchased from Sinopharm Chemical Reagent Co., Ltd. (Shanghai). All chemicals were of analytical reagent grade and used without further purification. Solutions were freshly prepared with deionized water.

S2. Synthesis of NiO@TiO₂

The synthesis procedure for NiO@TiO₂ is as follows: 1.5 mL Tetrabutyl titanate, 15 mL acetone and 15 mL hydrochloric acid were first dissolved into a 35 mL Teflon-lined stainless steel autoclave. A 1 cm × 2cm piece of clean carbon cloth (CC) treated with air plasma was immersed in the precursor solution in the autoclave. The autoclave was sealed and maintained at 150 °C for 5 h under self-generated pressure and then allowed to cool to room temperature naturally. The obtained TiO₂ nanorods on the CC were washed with deionized water and ethanol and dried at 80 °C in air. The double sides of as-prepared TiO₂ samples were further coated by NiO layers through radio-frequency magnetron sputtering. Finally, TiO₂ nanorods with NiO layer on carbon fibers were obtained. NiO layers were sputtered for 2 mins using a NiO ceramic target of 99.99% purity at different sputtering temperatures (100 °C: NiO@TiO₂-100 or NT-100; 200 °C: NiO@TiO₂-200 or NT-200; 300 °C: NiO@TiO₂-300 or NT-300; 400 °C: NiO@TiO₂-400 or NT-400). The working pressure kept 1 Pa, the sputtering power kept 60W and Ar flow rate maintained at 30sccm. The distance between target and substrate was 5cm throughout the sputtering process.

S3. Physicochemical characterization

Powder X-ray diffraction (XRD) patterns of the materials were obtained on a diffractometer (Bruker D8) using a Cu K α radiation source ($\lambda = 0.15418$ nm) with a 2θ scan from 10° to 90° with a step size of 0.04. X-ray photoelectron spectroscopy (XPS) was performed by a X-ray photoelectron spectrometer with a monochromatic Al K α source ($h\nu = 1486.6$ eV) and a charge neutralizer. All the binding energies were calibrated to the C 1s peak at 284.6 eV of the surface adventitious carbon. Scanning electron microscopy (SEM) images were collected using a Hitachi S-4800 microscope. High-resolution TEM (HRTEM) images were obtained using a Philips Tecnai 20U-Twin microscope at an acceleration voltage of 200 kV. The solution of samples was achieved after 20 min ultrasonic pretreatment. The TEM samples were prepared by dropping the primed solution onto a copper grid with polyvinyl formal support film and dried in air. ICP results were achieved by Agilent ICP-OES 730. Raman spectra were obtained using the LabRam HR system from Horiba Jobin Yvon at room temperature with a 514 nm solid laser as the exciting source. The electron spin resonance (ESR) signals were examined via a Bruker ER200-SRC spectrometer under visible light irradiation ($\lambda > 420$ nm).

S4. Computational Details

The density functional theory computations were carried out by Vienna ab initio simulation package (VASP) using the projector augmented wave (PAW) method [1-3]. The exchange correlation potential was represented by the Perdew–Burke–Ernzerhof (PBE) functional within the generalized gradient approximation (GGA) [4]. For the optimization of the lattice structure of bulk rutile TiO₂, the cutoff energy for the plane-

wave-basis expansion is set to be 500 eV, while the convergence tolerances of energy and force are set to 1.0×10^{-5} eV/atom and 10^{-3} eV/Å, respectively. The k -point sampling grid of TiO₂ and NiO are set to $6 \times 6 \times 10$ and $6 \times 6 \times 6$, respectively. Then, we cleave TiO₂ (110) and NiO (200) surfaces. Meanwhile, an oxygen vacancy (concentration is 3.23%) is formed on the surface of TiO₂ (110), which is abbreviated as TiO_{2-x}. Next, we used 2×2 supercell TiO_{2-x} (110) and 2×4 supercell NiO (200) surfaces to construct a heterostructure with a lattice mismatch of 4.39%, abbreviated as TiO_{2-x}/NiO. During structural optimizations, the bottom three layers atoms of TiO_{2-x} were fixed and the other atoms are relaxed. The cutoff energy was set to be 500 eV, and k -point sampling grid is $4 \times 2 \times 1$. The vacuum layer is set to 15 Å. The structures were relaxed until the convergence tolerances of energy and force were less than 1.0×10^{-5} eV/atom and 10^{-3} eV/Å. And, this work also used the DFT-D2 method to describe the van der Waals interaction^[5].

The ability of TiO_{2-x}/NiO to adsorb N₂ can be evaluated by calculating the adsorption energy (E_{abs}):

$$E_{\text{abs}} = E(\text{TiO}_{2-x}/\text{NiO} + \text{N}_2) - E(\text{TiO}_{2-x}/\text{NiO}) - E(\text{N}_2)$$

$E(\text{TiO}_{2-x}/\text{NiO} + \text{N}_2)$ and $E(\text{TiO}_{2-x}/\text{NiO})$ are the total energy of TiO_{2-x}/NiO adsorbed and unadsorbed N₂. $E(\text{N}_2)$ are the total energy of N₂ molecules.

The Gibbs free energy change (ΔG) of the elementary step was calculated by:

$$\Delta G = \Delta E + \Delta E_{\text{ZPE}} - T\Delta S - neU$$

Where ΔE represents the total energy difference, ΔE_{ZPE} and ΔS are the change in the zero-point energy and the entropy, respectively. U is the applied bias and in this work

is 0 eV. n is the number of electrons transferred during the reaction.

S5. Electrochemical testing

The electrocatalytic NRR tests were measured by using a two-compartment H-type like electrolytic cell, which was separated by a Nafion 117 membrane (DuPont). The Nafion membrane was pretreated by boiling it in H₂O₂ (5%) at 80 °C for 1h and deionized water for another 1h, sequentially. The electrochemical experiments were conducted with an electrochemical workstation (CHI 760C) by using a three-electrode configuration (working electrode of as-synthesized materials@CC, counter electrode of Pt plate, and reference electrode of Ag/AgCl/saturated KCl). Before NRR tests, the cathode electrolyte was purged with high purity nitrogen (99.999%, 40 mL/min) for 0.5 hour and then the flow rate was adjusted to 15 mL/min and maintained stable during the constant potential test for 3 hours. The NH₃ formation rate presented in the manuscript is the average data for the reaction of 3 hours. In this work, all potentials were converted to the reversible hydrogen electrode (RHE) potential using the equation given by $E_{\text{RHE}} = E_{\text{Ag/AgCl}} + 0.0591 \times \text{pH} + 0.194$, resulting in a shift of +0.6077V versus RHE (0.05 M Na₂SO₄, pH~7.1). Polarization curves were obtained using linear sweep voltammetry (LSV) with scan rate of 2 mV·s⁻¹ at 25 °C in the aqueous solutions (0.05 M Na₂SO₄) with constant N₂ (g) or Ar (g) continually purging for 30 min prior to the measurements. The polarization curves are the steady-state ones after several cycles. The long-term stability test was carried out using chronoamperometry measurements. A 300 W xenon lamp (PLS-SXE300C, Beijing Perfect Light Company) was used as the light source, providing UV-visible light throughout the control reaction procedure.

S6. Determination of NH₃

The concentration of produced NH₃ was spectrophotometrically detected by the indophenol blue method as previous reports.^[6-7] In detail, 2 mL aliquot of the solution was removed from the post-electrolysis electrolyte after reaction. Then 2 mL NaOH solution (1 M) containing 5 wt% salicylic acid and 5 wt% sodium citrate was added, followed by 1 mL 0.05 M NaClO and 0.2 mL 1 wt% sodium nitroferricyanide (C₅FeN₆Na₂O) solution. After 1h, the absorption spectra of the mixed solution were measured with an ultraviolet-visible spectrophotometer. The concentration of NH₃ was determined by absorbance at a wavelength of ~655 nm. Absolute calibration was achieved using NH₄⁺ of known concentration in 0.01 M HCl solutions as standards. The concentration of NH₃ were determined by a standard curve (Absorbance = 1.068 × c_{NH3} + 0.086, R² = 0.999).

S7. Calculations of NH₃ yield and Faradaic efficiency

The NH₃ yield was calculated using the following equation:

$$Yield(NH_3) = \frac{c_{NH_3} \times V}{17 \times t \times A}$$

where c_{NH3} is the measured NH₃ concentration (μg mL⁻¹), V is the volume of the electrolyte solution (10 mL), t is the reaction time (3 h), A is the area of the work electrode (2 cm²). The Faradaic efficiency (FE) for NRR was defined as the quantity of electric charge used for synthesizing NH₃. The production of NH₃ molecule theoretically need three electrons. The FE was calculated by the following equation:

$$FE = \frac{3F \times c_{NH_3} \times V}{17 \times I \times t} \times 100\%$$

Where F is Faraday constant ($96485 \text{ C}\cdot\text{mol}^{-1}$), c_{NH_3} is the measured NH_3 concentration ($\mu\text{g mL}^{-1}$), V is the volume of the electrolyte solution (10 mL), I is the current (A), t is the reaction time (3 h).

S8. ^{15}N isotope labeling experiments

Isotope labeling static experiments with $^{15}\text{N}_2$ (from Anze special gas, Zibo) as feed gas were conducted to clarify the source of NH_3 . The reactor was previously encapsulated and degassed with argon for several times, and subsequently filled with $^{15}\text{N}_2$. After NRR procedure, the obtained $^{15}\text{NH}_4^+$ electrolyte (0.1 mL, concentrated electrolyte) was thoroughly mixed with 0.5 mL dimethyl sulphoxide- D_6 and 0.1 mL D_2O for the ^1H nuclear magnetic resonance (NMR) test on a Bruker Avance spectrometer (500 MHz). For comparison, $^{14}\text{N}_2$ experiment was also operated in the same way.

S9. Supplementary figures and tables

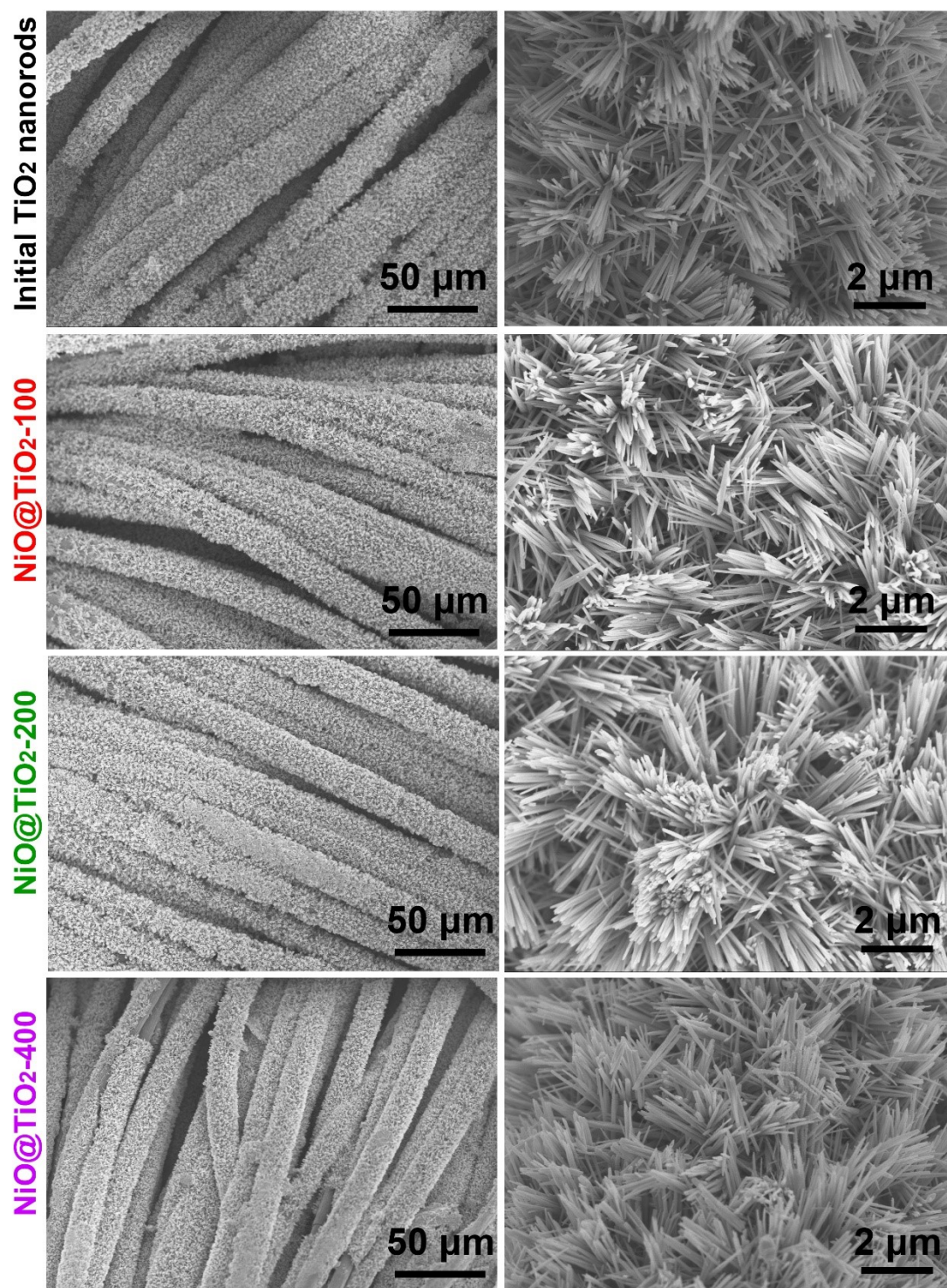


Figure S1. SEM images of initial TiO₂ and NiO@ TiO₂ control samples.

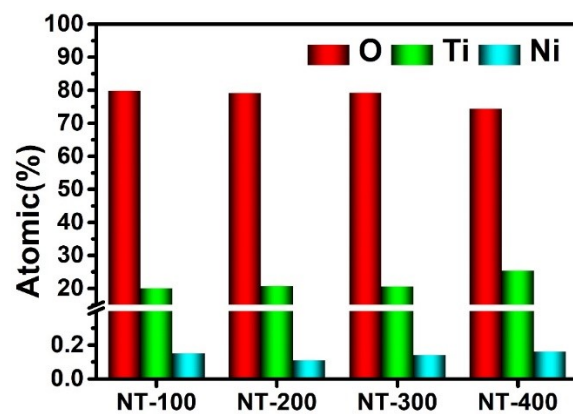


Figure S2. EDS elements analyses of NiO@TiO₂ prepared at different magnetron sputtering temperatures.

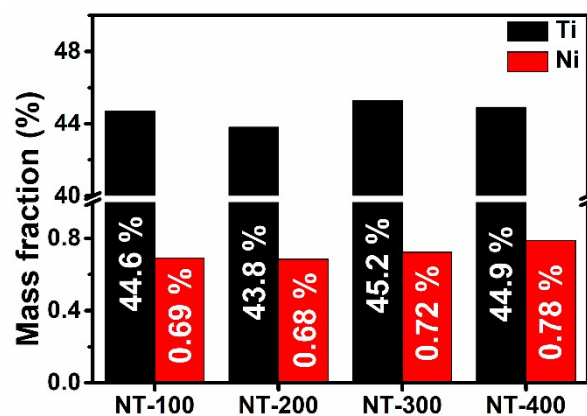


Figure S3. ICP-MS analyses of NiO@TiO₂ prepared at different magnetron sputtering temperatures.

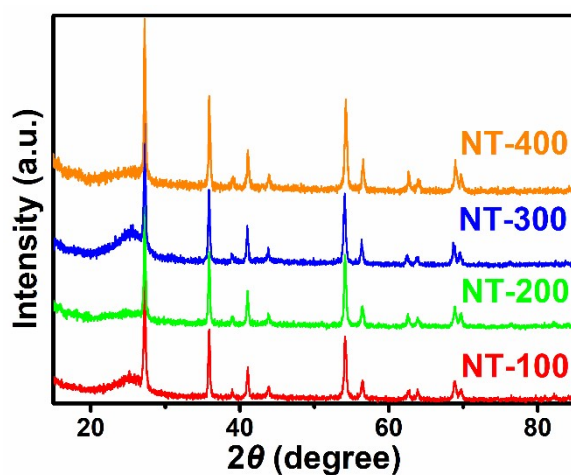


Figure S4. XRD patterns of NiO@TiO₂ prepared at different magnetron sputtering temperatures.

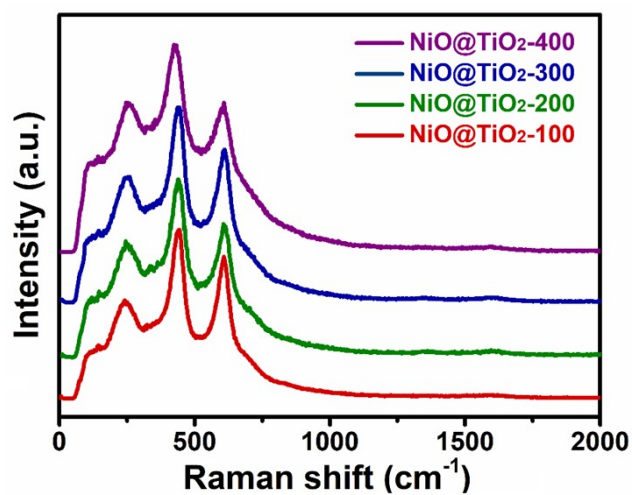


Figure S5. Raman scattering spectra of NiO@TiO₂ prepared at different magnetron sputtering temperatures.

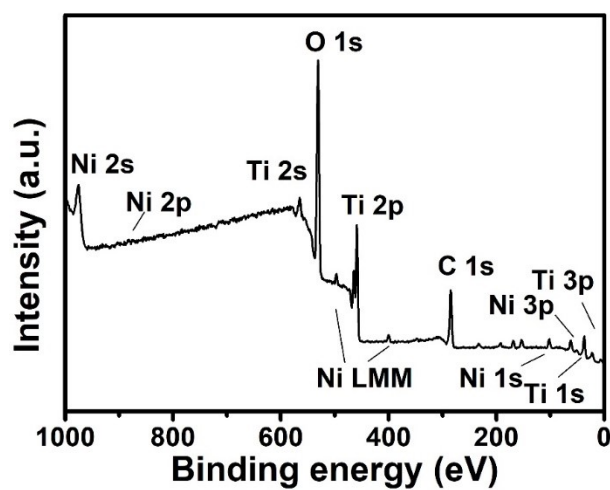


Figure S6. The survey XPS spectrum of as-synthesized NiO@TiO₂.

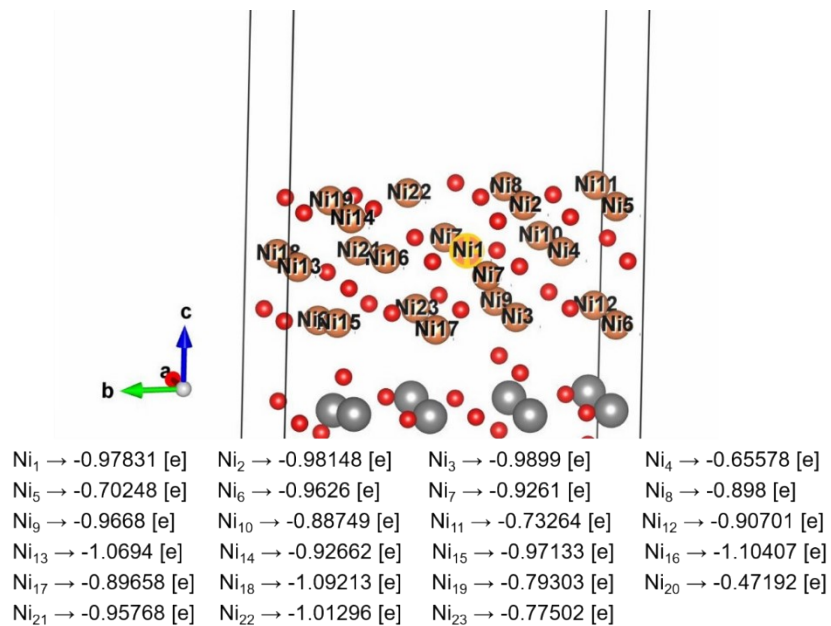


Figure S7. The side view of the local structure of Ni_{1-x}O@TiO_{2-x}. The Bader charges carried by Ni atoms labeled with numbers are shown below the figures.

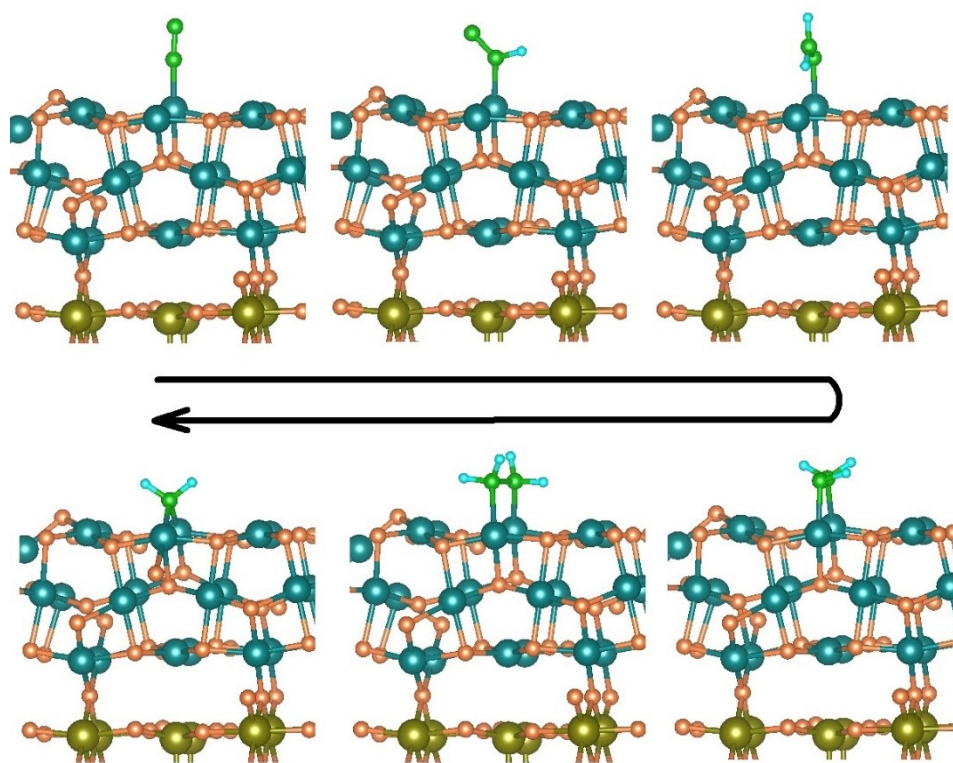


Figure S8. The structures of intermediate adsorption on NiO@TiO₂ for side reaction.

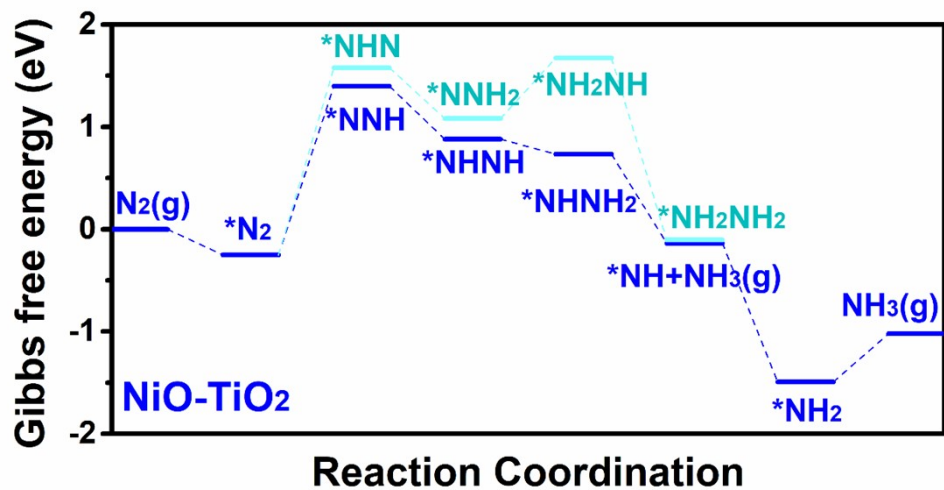


Figure S9. Free energy diagram for NRR on NiO@TiO₂.

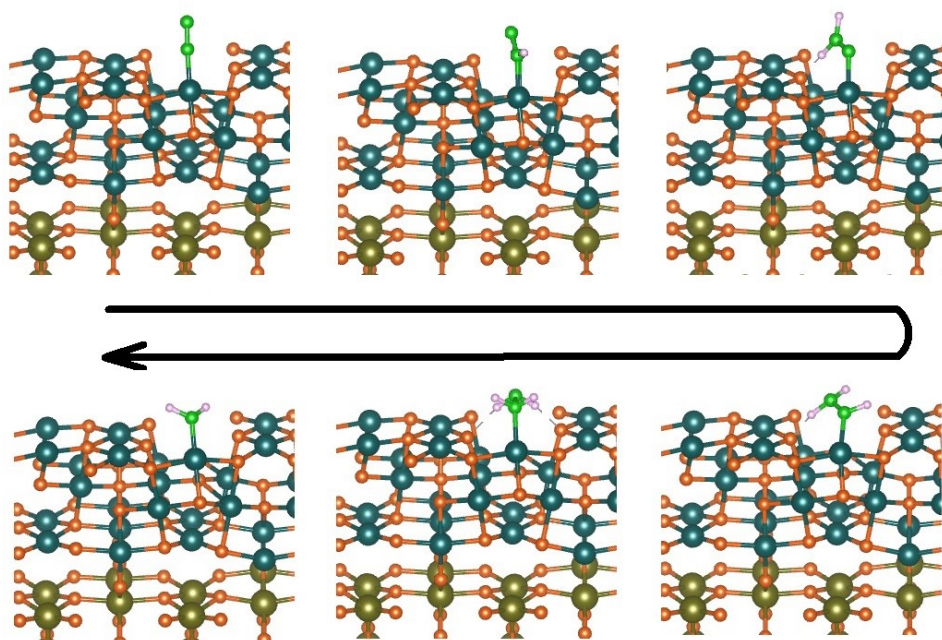


Figure S10. The structures of intermediate adsorption on Ni_{1-x}O@TiO_{2-x} for side reaction.

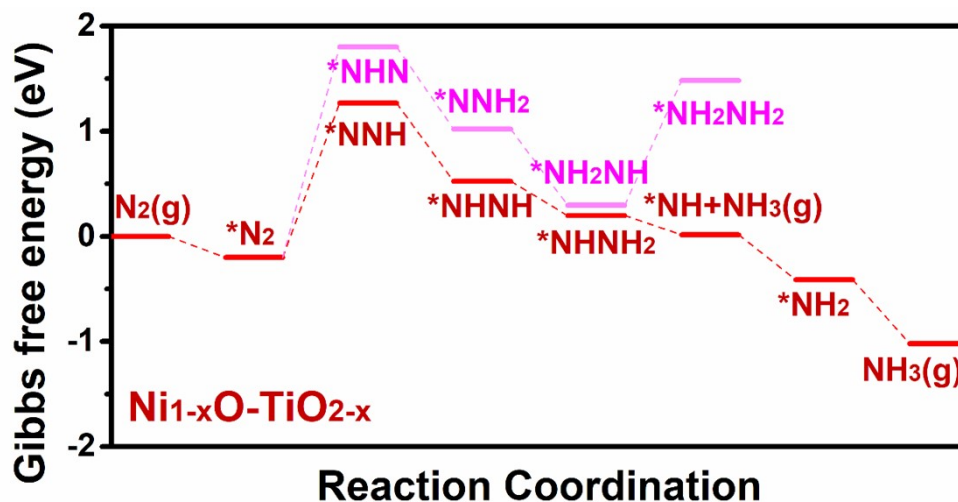


Figure S11. Free energy diagram for NRR on $\text{Ni}_{1-x}\text{O}@\text{TiO}_{2-x}$.

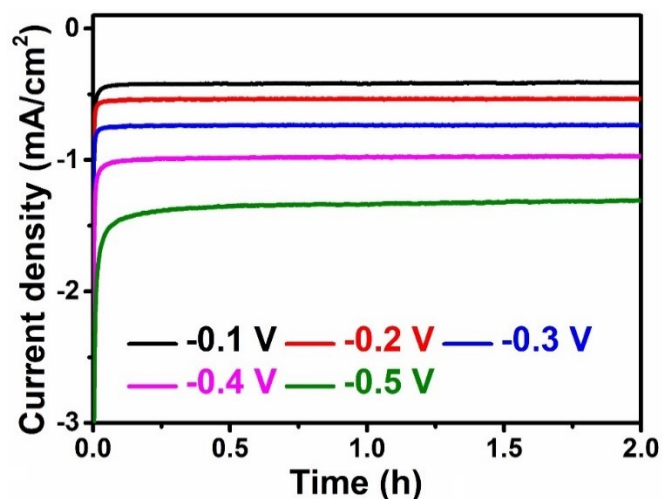


Figure S12. The chrono-amperometry curves for $\text{NiO}@\text{TiO}_2$ at various potentials.

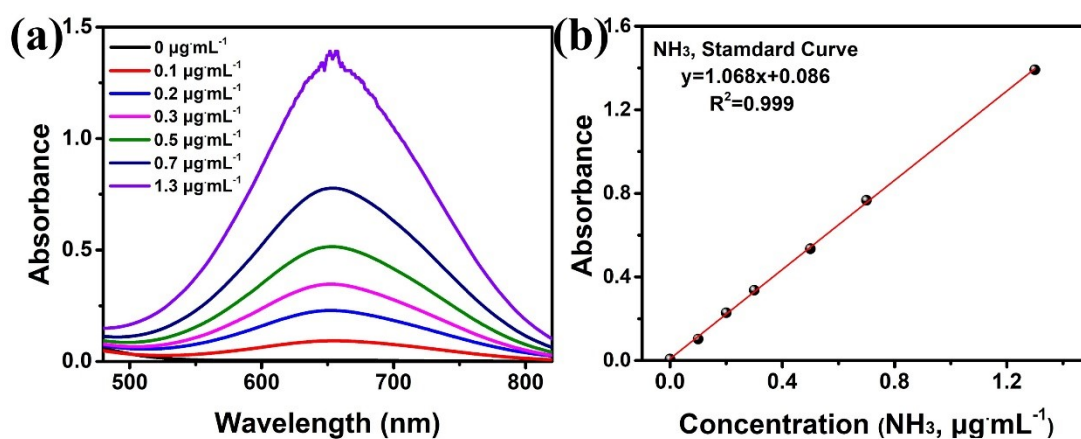


Figure S13. Calibration of the indophenol blue method using a series of NH_4Cl standard solutions. (a) UV-vis curves of indophenol assays with NH_4^+ ions, (b) calibration curve used for estimation of NH_3 from the NH_4^+ ion concentration.

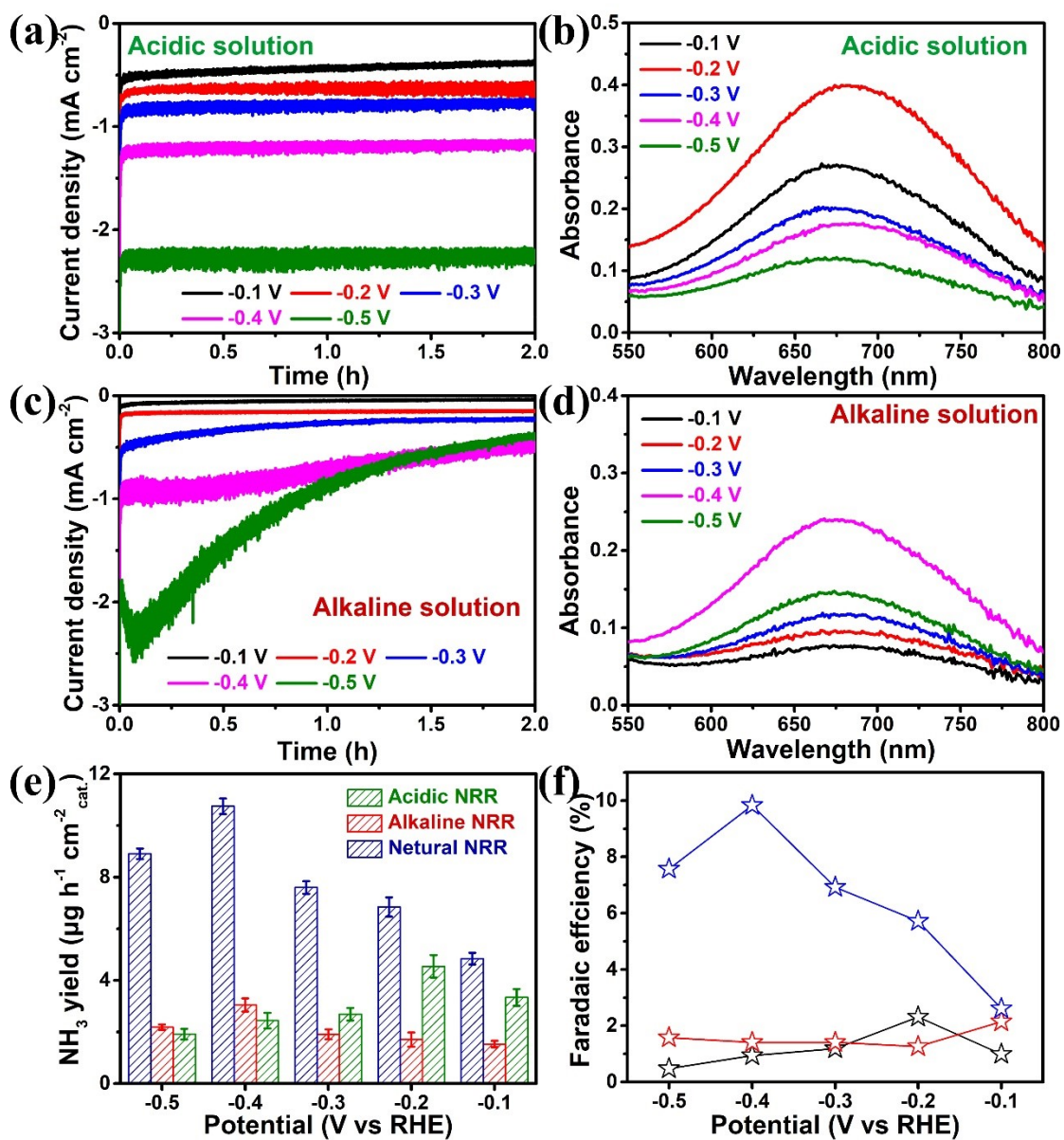


Figure S14. Chronoamperometry curves of NiO@TiO₂-300 at various potentials for 2 hours in N₂-saturated acidic (a) and alkaline (c) electrolyte. UV-vis absorption spectra of the electrolytes using NiO@TiO₂-300 after acidic (b) and alkaline (d) NRR electrocatalysis. Comparison of NH₃ yields (e) and FEs (f) of NiO@TiO₂-300 in different solutions.

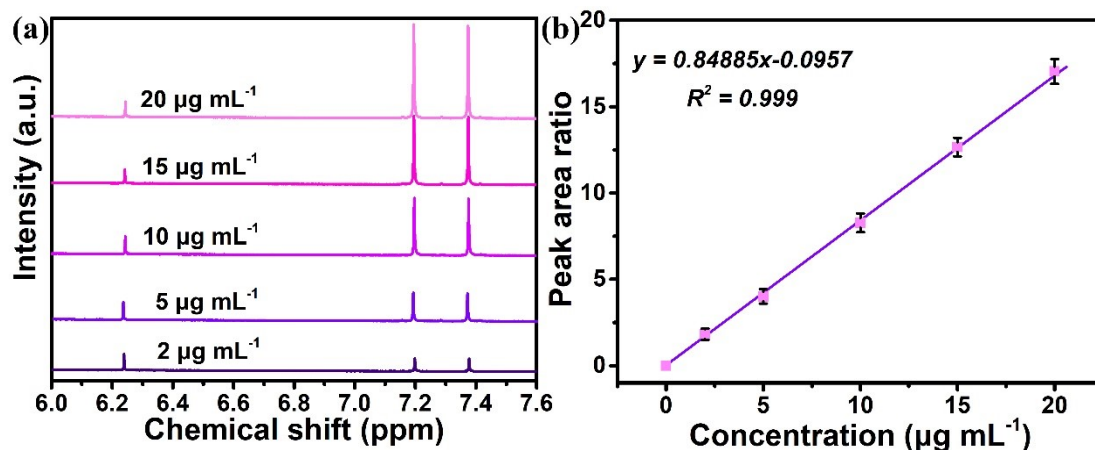


Figure S15. (a) ¹H NMR spectra of different ¹⁵NH₄⁺ concentrations. (b) Integral area ratio (¹⁵NH₄⁺/C₄H₄O₄) against ¹⁵NH₄⁺ concentration. The error bars correspond to the standard deviations of measurements over three separately prepared samples under the same conditions.

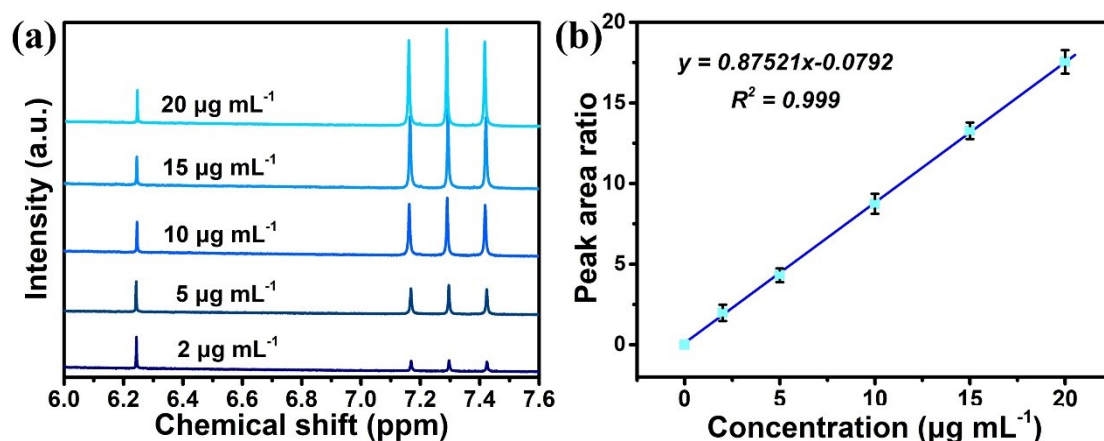


Figure S16. (a) ¹H NMR spectra of different ¹⁴NH₄⁺ concentrations. (b) Integral area ratio (¹⁴NH₄⁺/C₄H₄O₄) against ¹⁴NH₄⁺ concentration. The error bars correspond to the standard deviations of measurements over three separately prepared samples under the same conditions.

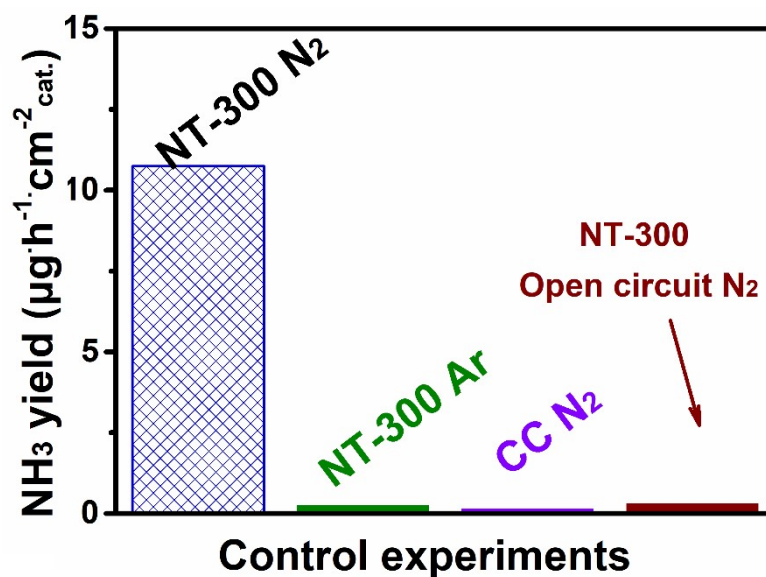


Figure S17. NH_3 yields of control experiments under Ar atmosphere, over bare CC or driven at open circuit.

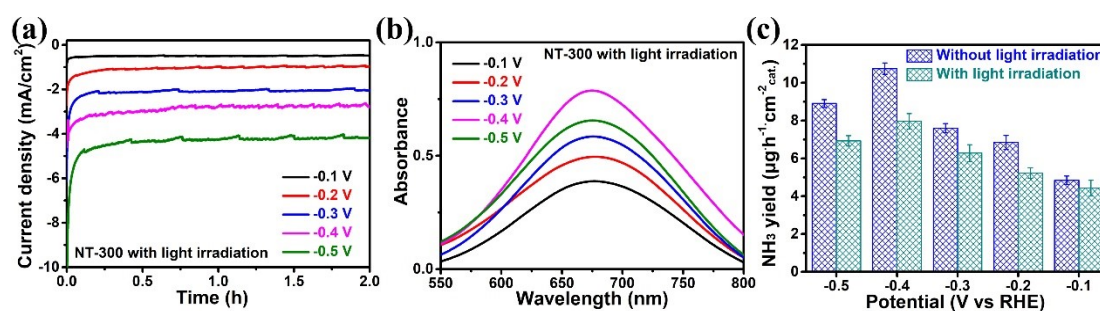


Figure S18. The chrono-amperometry curves for $\text{NiO}@\text{TiO}_2\text{-300}$ with light irradiation (a). UV-Vis absorption spectra of the electrolytes stained with indophenol indicator at various potentials of reprepared $\text{NiO}@\text{TiO}_2\text{-300}$ with light irradiation (b). The comparison of NH_3 yields over $\text{NiO}@\text{TiO}_2\text{-300}$ with or without light irradiation (c).

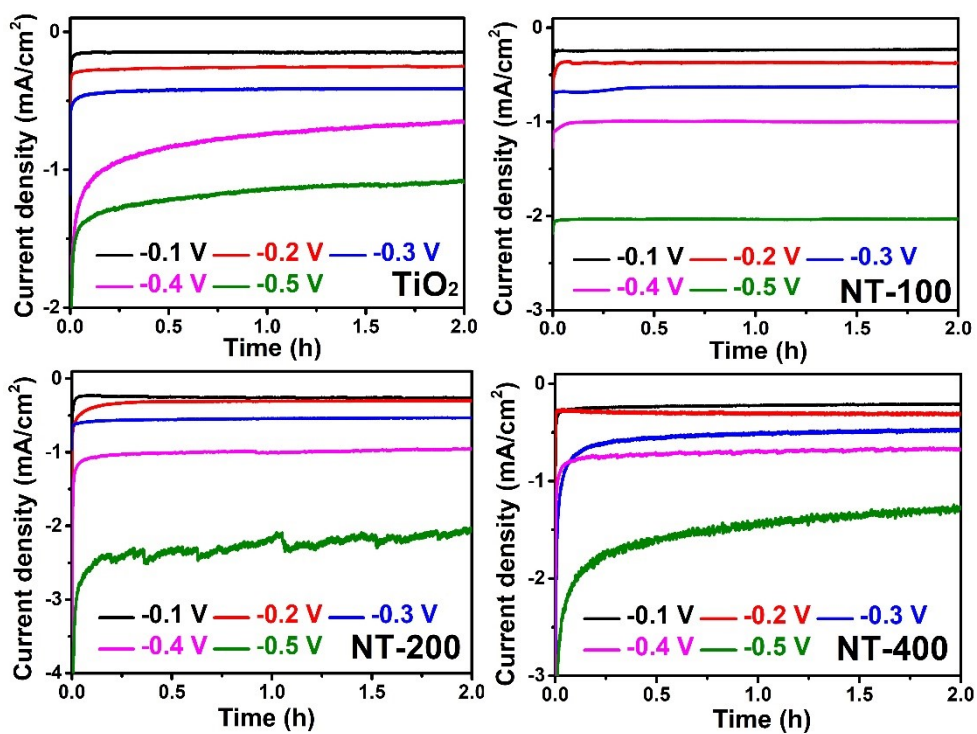


Figure S19. The chrono-amperometry curves of (a) pristine TiO₂, (b) NiO@TiO₂-100, (c) NiO@TiO₂-200 and (d) NiO@TiO₂-400.

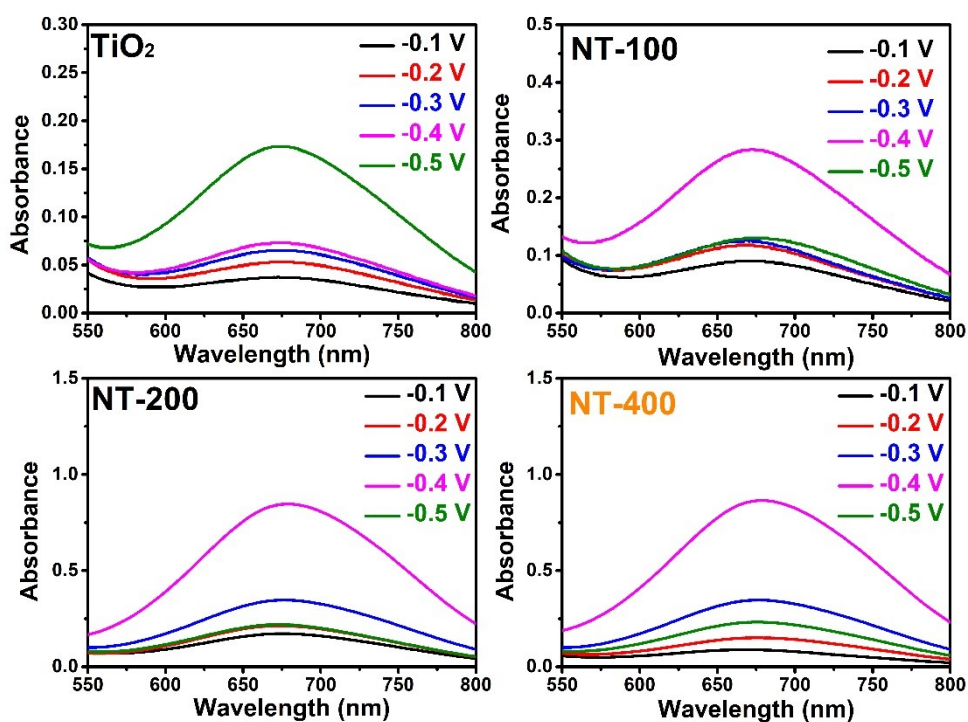


Figure S20. UV-Vis absorption spectra of the electrolytes stained with indophenol indicator at various potentials of (a) pristine TiO₂, (b) NiO@TiO₂-100, (c) NiO@TiO₂-

200 and (d) NiO@TiO₂-400.

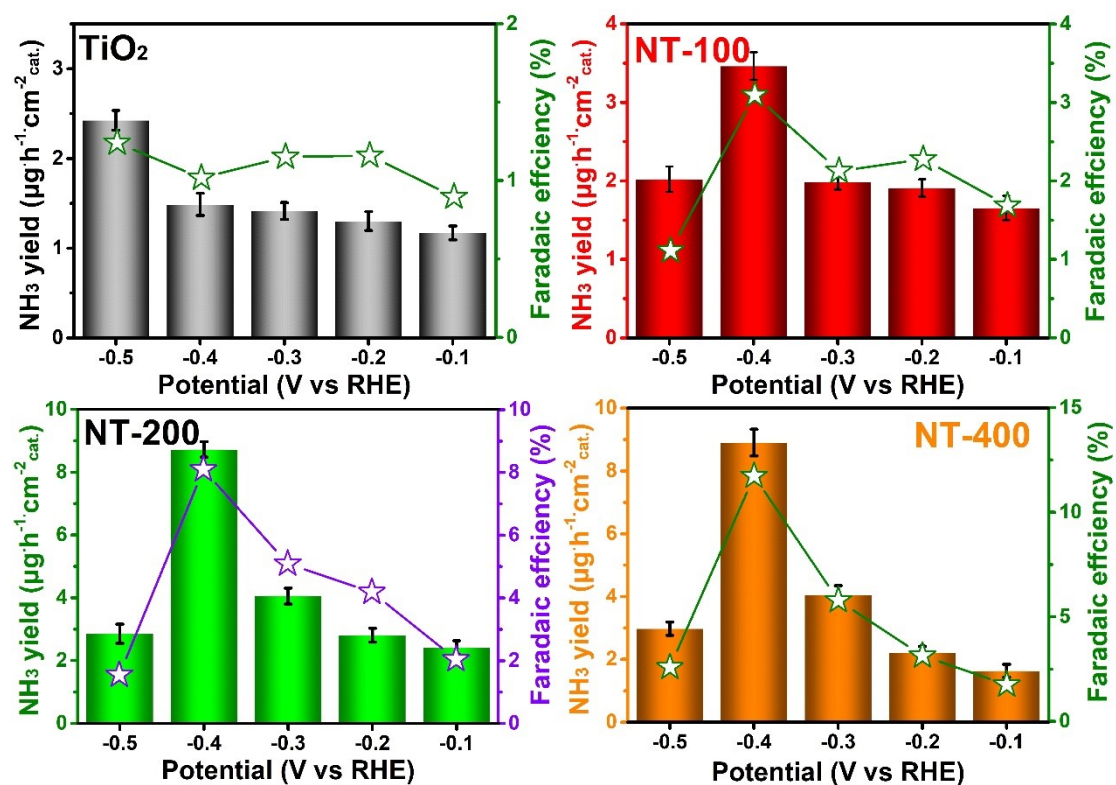


Figure S21. NH₃ yields and FEs at various potentials over (a) pristine TiO₂, (b) NiO@TiO₂-100, (c) NiO@TiO₂-200 and (d) NiO@TiO₂-400.

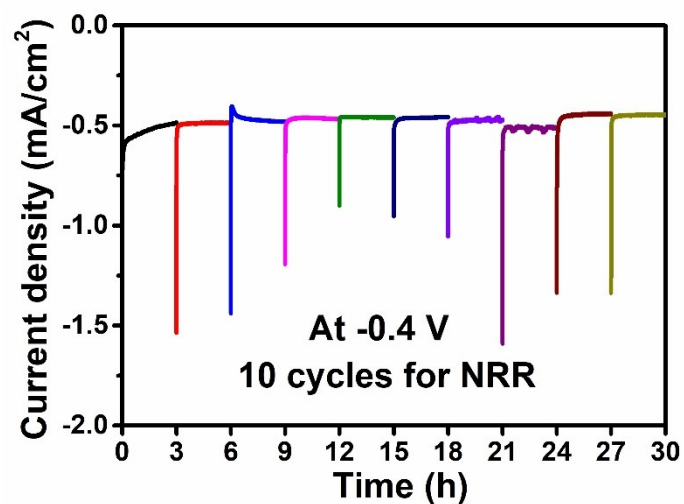


Figure S22. Cycling test of chrono-amperometry curves using NiO@TiO₂-300 at -0.40 V vs. RHE.

Table S1. Summary of neutral NRR performances of different catalysts.

| Catalyst | Electrolyte | NH ₃ yield ($\mu\text{g}\cdot\text{h}^{-1}\cdot\text{cm}^{-2}_{\text{cat.}}$) | Overpotential (vs. RHE) | FE (%) | Reference |
|---|--|---|----------------------------|----------------------|--|
| NiO@TiO₂ | 0.05 M Na₂SO₄ | 10.75 | -0.40 | 9.83 (-0.4 V) | This work |
| CoS ₂ -CeO ₂ /Ti | 0.10 M Na ₂ SO ₄ | 22.37 | -0.50 | 2.52 (-0.5 V) | <i>ACS Sustainable Chem. Eng.</i> 2021 , 9, 13399 |
| VNiON | 0.05 Na ₂ SO ₄ | 6.78 | -0.40 | 5.57 (-0.2 V) | <i>J. Mater. Chem. A</i> , 2020 , 8, 91 |
| Zr-doped TiO ₂ | 0.10 M Na ₂ SO ₄ | 8.9 | -0.45 | 17.3 (-0.45 V) | <i>Nature Commun.</i> , 2019 , 10, 2877 |
| V ₂ O ₃ /C | 0.10 M Na ₂ SO ₄ | 12.3 | -0.60 | 7.28 (-0.6 V) | <i>Inorg. Chem. Front.</i> 2019 , 6, 391 |
| TiO ₂ /Ti | 0.10 M Na ₂ SO ₄ | 5.6 | -0.70 | 2.50 (-0.7 V) | <i>ACS Appl. Mater. Interfaces</i> 2018 , 10, 28251 |
| MoS ₂ /CC | 0.10 M Na ₂ SO ₄ | 4.94 | -0.50 | 1.17 (-0.5 V) | <i>Adv. Mater.</i> 2018 , 30, 1800191 |
| Y ₂ O ₃ nanosheet | 0.10 M Na ₂ SO ₄ | 6.49 | -0.90 | 2.53 (-0.9 V) | <i>Ind. Eng. Chem. Res.</i> 2018 , 57, 16622 |
| SnO ₂ /CC | 0.10 M Na ₂ SO ₄ | 9.0 | -0.80 | 2.17 (-0.7 V) | <i>Chem. Commun.</i> 2018 , 54, 12966 |

References

- [1] G. Kresse, D.J. Joubert, From ultrasoft pseudopotentials to the projector augmented wave method, *Phys. Rev.* 59 (1999) 1758.
- [2] G. Kresse, J. Furthmüller, Efficiency of ab-initio total energy calculations for metals and semiconductors using a plane-wave basis set, *Comp. Mater. Sci.* 6 (1996) 15-50.
- [3] G. Kresse, J. Furthmüller, Efficient iterative schemes for ab initio total-energy calculations using a plane-wave basis set, *Phys. Rev.* 54 (1996) 11169.
- [4] J.P. Perdew, K. Burke, M. Ernzerhof, Generalized gradient approximation made simple, *Phys. Rev. Lett.* 77 (1996) 3865.
- [5] S. Grimme, J. Antony, S. Ehrlich, H. Krieg, A consistent and accurate ab initio parametrization of density functional dispersion correction (DFT-D) for the 94 elements H-Pu. *J. Chem. Phys.* 132 (2010) 154104
- [6] Du H, Guo X, Kong R M, et al. Cr₂O₃ nanofiber: a high-performance electrocatalyst toward artificial N₂ fixation to NH₃ under ambient conditions. *Chemical Communications*, 2018, 54(91): 12848-12851.
- [7] Jia K, Wang Y, Qiu L, et al. TiS₂ nanosheets for efficient electrocatalytic N₂ fixation to NH₃ under ambient conditions. *Inorganic Chemistry Frontiers*, 2019, 6(8): 1986-1989.